Fast Ambiguity Resolution for Marine Navigation

Falin WU *, Nobuaki KUBO** and Akio YASUDA**

ABSTRACT

Precise positioning using GPS carrier phase measurement has been widely used in static applications. However, it can also been applied to precise positioning of a moving platform if ambiguities contained in the GPS carrier phase measurement are resolved during the motion. Precise positioning of a ship is especially difficult due to the high dynamics of the antenna and the high reflectivity of the water. However, marine application can use altitude aiding to help significantly in resolving the ambiguities. In this paper, a new approach for ambiguity resolution method using altitude aiding and wide-lane search before stepping to L1 ambiguity search technique in the marine environment is investigated. The algorithm has been tested in Tokyo Bay. The ambiguity fixed percentages are 95.3% without altitude aiding and 97.5% with altitude aiding. The time to fix is almost single epoch with altitude aiding.

1. Introduction

GPS positioning is required for a variety of navigation and hydrographic applications. In order to achieve the centimeter level accuracy, carrier phase measurements must be employed. Carrier phase measurements are precise but they are ambiguous because the number of whole cycles between the satellite and the receiver is unknown. Thus, this unknown cycle of carrier phase observables must be correctly resolved in kinematic positioning.

Precise positioning of a moving ship is especially difficult due to the high dynamics of the antenna and the high reflectivity of the water. Ambiguity resolution on-the-fly is not easy to be achieved. It relies on a lot of factors, such as ambiguity search techniques, a change in satellite geometry, and the effects of the observation error. In the marine environment, the ship dynamics is generally more turbulent, cycle slips are more frequent, multipath caused by the ship's reflective structure and sea water is much large, and the ship can never be static even if anchored in harbor. Therefore, on-the-fly ambiguity resolution is more difficult at the beginning of the session, cycle slip occurrences as well as on occasions when the rising of a new satellite will be included in the positioning process.

This paper addresses the development of ambiguity resolution in marine environment. For completeness, a short description of the observation models is presented. This is followed by the description of ambiguity resolution algorithm. Tests and results of the new approach are presented. Finally concluding remarks and proposals for future research are given.

2. Fast Ambiguity Resolution Algorithm

In this section, a general view of observation models is given, and then fast ambiguity resolution algorithm is introduced.

2.1 Observation Models

Four basic observables are available from the GPS satellites, the code and carrier measurements on the L1 and L2 frequencies. These observables can be combined in several ways, giving different observation models and methods for ambiguity resolution

2.1.1 Double Difference

The double difference observables are[3]

$$P_1 = r + e_I + e_T + e_{m_{p_1}} + e_1 \quad (1)$$

$$P_2 = r + (l_2 / l_1)^2 e_I + e_T + e_{m_{p_2}} + e_2 \quad (2)$$

$$\Phi_1 = r - e_I + e_T + e_{m_{f_1}} + l_1 N_1 + e_1 \quad (3)$$

$$\Phi_2 = r - (l_2 / l_1)^2 e_I + e_T + e_{m_{f_2}} + l_2 N_2 + e_2 \quad (4)$$

where Φ_i and P_i are double difference carrier phase and pseudorange, respectively; l_i is the carrier wavelength; r is the double difference geometric range from receiver to the GPS satellite; N_i is ambiguity; e_I and e_T are the

* Student Member: Tokyo University of Mercantile Marine (2-1-6 Etchujima, Koto-ku, Tokyo 135-8533)
** Member: Tokyo University of Mercantile Marine (2-1-6 Etchujima, Koto-ku, Tokyo 135-8533)

double difference delays due to the ionosphere and the troposphere, respectively; $e_{m_{fi}}$ and $e_{m_{Pi}}$ represent the double difference effect of multipath on the carrier phases and the pseudoranges, respectively; e_i and e_i represent the double difference effect of receiver noise on the carrier phases and the pseudoranges, respectively.

2.1.2 Linear Combinations of observables

Some kinds of linear combinations of observables can be formed, which are useful for the ambiguity resolution on-the-fly and cycle slip detection. The most common combinations are the wide and narrow-lane observables and the ionospheric-free and ionospheric-signal combinations.

The wide and narrow-lane combinations are

$$\begin{aligned}\Phi_W &= \left(\frac{\Phi_1}{l_1} - \frac{\Phi_2}{l_2}\right) l_W \\ &= r + (l_2 / l_1) e_I + e_T + e_{m_{fW}} + l_W N_W + e_W\end{aligned} \tag{5}$$

$$\begin{aligned}\Phi_N &= \left(\frac{\Phi_1}{l_1} + \frac{\Phi_2}{l_2}\right) l_N \\ &= r - (l_2 / l_1) e_I + e_T + e_{m_{fN}} + l_N N_N + e_N\end{aligned} \tag{6}$$

where $N_W = N_1 - N_2$ and $N_N = N_1 + N_2$ are ambiguities of wide and narrow-lane respectively; $l_W = l_1 l_2 / (l_2 - l_1) \cong 86.2cm$ and $l_N = l_1 l_2 / (l_2 + l_1) \cong 10.7cm$ are wave-length of wide and narrow-lane respectively.

The wavelength of wide-lane is about four times as large as L1 wavelength, to resolve wide-lane ambiguities is easier than for L1 ambiguities.

The carrier ionospheric-free and ionospheric-signal combinations are

$$\begin{aligned}\Phi_{ion} &= (\Phi_W + \Phi_N)/2 \\ &= r + (l_N N_N + l_W N_W)/2 + e_T + e_{m_{fion}} + e_{ion}\end{aligned} \tag{7}$$

$$\begin{aligned}\Phi_I &= \Phi_N - \Phi_W \\ &= -2(l_2 / l_1) e_I + l_N N_N - l_W N_W + (e_{m_N} - e_{m_W}) + (e_N - e_W)\end{aligned} \tag{8}$$

The ionospheric-free combination has its main application for long baseline positioning, where the ionosphere is difficult to model with sufficient accuracy. The ionospheric-signal combination has been suggested for cycle-slip detection.

2.2 Ambiguity Resolution On-the-Fly

The purpose of ambiguity resolution is to determine the L1 and/or L2 ambiguity. However, the wide-lane ambiguity could be resolved before stepping to L1 ambiguity resolution. Furthermore, the carrier-smoothed pseudorange is also used to determine the initial value of wide-lane ambiguity. The flowchart of ambiguity resolution algorithm is shown in Figure 1. The details are described step by step as follows.

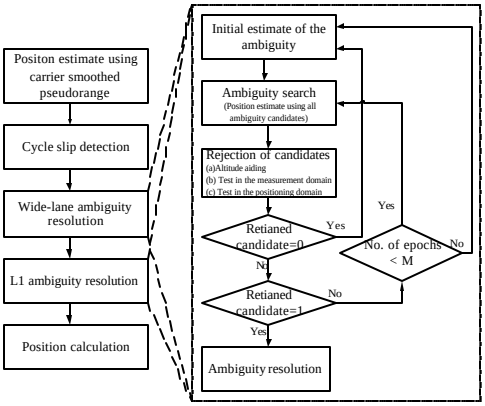

Figure 1. Flowchart of the OTF algorithm

2.2.1 Cycle-Slip Detection

When dealing with carrier phase measurements, one of the first steps regarding its processing is to detect the cycle-slips that eventually might happen due to several causes. Cycle slips can be easily detected for dual frequency by monitoring the inospheric-signal in Equation (8). Taking the time difference of the ionospheric-signal and denoting it, $\Phi_I(t_n) - \Phi_I(t_{n-1})$. If a cycle slip occurs in the L1 and/or L2 carriers as dN_1 and dN_2, $\Phi_I(t_n) - \Phi_I(t_{n-1})$ will jump as[2]

$$\begin{aligned}&\Phi_I(t_n) - \Phi_I(t_{n-1}) \\ &= -2(l_2 / l_1)\{e_I(t_n) - e_I(t_{n-1})\} + (l_N - l_W) dN_1 + (l_N + l_W) dN_2 \\ &\cong -2(l_2 / l_1)\{e_I(t_n) - e_I(t_{n-1})\} - 75.5 \cdot dN_1 + 96.9 \cdot dN_2 (cm)\end{aligned} \tag{9}$$

where the multipath and measurement noise are omitted. Therefore, the cycle slip in the L1 or L2 carrier would be easily detected by using a threshold value.

2.2.2 Wide-lane Ambiguity Resolution

Procedure 1. Define Search Grid

The initial estimates of wide-lane ambiguities are determined by Equation (10) using the position of the receiver, which is calculated using the double differences of carrier smoothed L1 pseudorange [3].

$$\hat{N}_W = \left[\frac{f_W - r - e_T}{l_W}\right]_{roundoff} \tag{10}$$

where r are the double differenced geometrical distances from the receiver to satellites, r are calculated using carrier-smoothing pseudorange-position. The notation "*roundoff*" means to make the nearest integer. The correct integer ambiguity should be in a domain centered to the initial value shown in the following equation:

$$\hat{N}_w^i - k s_N^W \le N_W^i \le \hat{N}_w^i + k s_N^W \quad (i = 1,2,\cdots,nsv-1) \tag{11}$$

where *nsv* is number of observed satellites, and s_N^W denotes the standard deviation of initially estimated wide-lane ambiguity. k is the desired level of confidence, k=2 and 3 correspond to the confidence level of 95% and 99%, respectively. The standard deviation of the initially estimated ambiguity s_N^W is

$$\begin{aligned} s_N^W &= \sqrt{\left(s_m^{PR}\right)^2 + \left(s_m^W\right)^2} \\ &= \sqrt{65^2 + 4^2} \cong 65cm \end{aligned} \tag{12}$$

where s_m^{PR} and s_m^W are the standard deviations of smoothed pseudoranges and wide-lane measurements, respectively.

To minimum the ambiguity search space, the observables could be separated into groups of primary and secondary. The primary observables should ideally be chosen to optimize RDOP (relative Dilution of Precision). Using the RDOP, the standard deviation of double differenced measurement error s_m and positioning error s_p satisfy the following relation:

$$s_p = RDOP s_m \tag{13}$$

If three ambiguities of primary satellites are resolved, the position of the user receiver is obtained. Therefore, the ambiguities of secondary satellites can be computed by inserting the position calculated using ambiguities of primary observables instead of the pseudorange-position into r of the right side of Equation (10). The ambiguities of primary observables are firstly resolved by the least squares searching method, and the ambiguities of the secondary satellites are resolved next.

Because the wavelength of wide-lane is about 86cm, the solution is in a range of initial value ± 2 cycles with a confidence level of 99%. The search number would be $5^3 = 125$.

Procedure 2. Ambiguities Search

Receiver position is computed with each ambiguity candidate First altitude aiding is used to perform rejection of candidate, then the statistical tests are performed in the measurement domain and positioning domain.

(a) Candidate rejection using altitude aiding

Altitude can be used to help in resolving the ambiguities[4]. The candidates satisfied the following conditions are rejected:

$$A^W > A_{\max} \quad or \quad A^W < A_{\min} \tag{14}$$

where A^W denotes the altitude of antenna calculated using wide-lane. A_{max} and A_{min} denote the maximum and minimum altitude respectively. A_{max} and A_{min} can be calculated from water level information and other information, but in this paper, A_{min} and A_{max} are calculated from the result of Marine-VRS test. The Marine-VRS test will be described in the Section 3.

Figure 2 shows the altitude variation when experiment ship sailed from Tokyo University of Mercantile Marine (TUMM) to Rainbow Bridge at Tokyo Bay. The time is about 30 minutes. The average and standard deviation of altitude are 40.439m and 6.77cm, respectively. In this paper, A_{min} and A_{max} are set to 39.8m and 41.2m, respectively.

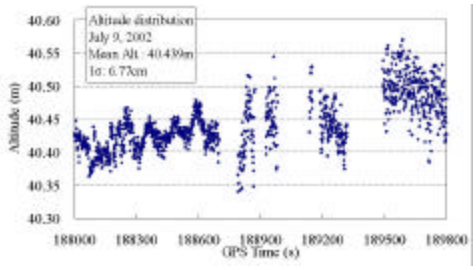

Figure 2. Variation of Altitude

(b) Test in the measurement domain

The c^2 test is performed using the sum of measurement residuals. The candidates satisfying the following condition are rejected[2]:

$$\frac{v^T C_W^{-1} v}{df} > \frac{c_{df,1-a}^2}{df} k_1^W \tag{15}$$

where v, a and df denote the residual vector, the confidence level of the c^2 test, and the degree of freedom (=nsv-4), respectively. k_1^W is an empirical parameter of tolerance, which is set to 1~2 in the experiments considered.

(c) Test in the positioning domain

Taking the differences between the horizontal positions computed using smoothed pseudoranges and those using each ambiguity candidate, the candidates satisfy the following condition are rejected[2]:

$$\left| r^{PR} - r^{W} \right|_H > k_2^W s_H^{PR-W} \qquad (16)$$

where r^{PR} and r^{W} denote the position vectors of antenna calculated using smoothed pseudorange and wide-lane, respectively, and $\left| \cdot \right|_H$ means to take the horizontal norm. s_H^{PR-W} shows the standard deviation of the difference between the pseudorange-position and the wide-lane-position in the horizontal. k_2^W is an empirical parameter of the tolerance, theoretically, k_2^W =1, 2, 3 corresponds to the confidence level of 68%, 95%, 99%, respectively.

The standard deviation of the difference between the pseudorange-position and wide-lane-position is given as follows

$$s_H^{PR-W} = RHDOP\sqrt{\left(s_m^{PR}\right)^2 + \left(s_m^{W}\right)^2} \qquad (17)$$
$$= RHDOP\sqrt{65^2 + 4^2} \cong 65 \cdot RHDOP(cm)$$

Procedure 3: If one ambiguity candidate set is retained, that is considered as the solution; if more than one candidate are retained, similar tests will be performed at the next epoch.

The tests shown in Equation (14), (15) and (16) are called local tests, because measurement data of a single epoch are used. In addition to the local tests, the global tests that use the data of multiple epochs are performed.

Procedure 4: *Procedure 2* and *Procedure 3* are repeated until only one candidate is retained. If the number of total epochs exceeds a threshold number, M, the process returns to *Procedure 1*.

2.2.3 L1 Ambiguity Resolution

The procedure of L1 ambiguity resolution is similar to the procedure of wide-lane ambiguity resolution.

The initial values of L1 ambiguity are calculated from the wide-lane-position. The standard deviation of initially estimated L1 ambiguity, s_N^{L1} is

$$s_N^{L1} = \sqrt{\left(s_m^{W}\right)^2 + \left(s_m^{L1}\right)^2} \cong 4cm \qquad (18)$$

Because the L1 wavelength is 19cm, the solution will be in a range of initial ambiguity ± 1 cycle (99%). And the search number is $3^3 = 27$.

In the case of L1 ambiguity resolution, the test in positioning domain is very powerful. The standard deviation of the difference between the wide-lane-position and L1-position is given by the next equation

$$s_H^{W-L1} = RHDOP\sqrt{\left(s_m^{W}\right)^2 + \left(s_m^{L1}\right)^2} \qquad (19)$$
$$\cong 4 \cdot RHDOP\ (cm)$$

3. Test Results

For testing the algorithm, experiment, namely Marine-RTK and Marine-VRS have been conducted on July 9, 2002 in Tokyo Bay. Marine-RTK uses the algorithm proposal in this paper. Marine-VRS is conducted using Virtual Reference System (VRS) [1]. VRS uses a network of reference stations to isolate the systematic effects of ephemeris, tropospheric and ionospheric errors, and use the resultant corrections to create a Virtual Reference Station at any location within the network. Use of VRS significantly reduces the effects of systematic error and allows wider coverage, higher reliability, improved accuracy and lower initialization times than can be achieved by classical RTK techniques.

3.1 Set-up of tests

Figure 3 shows the set-up of the Marine-RTK and Marine-VRS experiment. The antenna of Marine-RTK reference is installed at a fixed point on the top of a building in TUMM. The only one rover antenna is settled on the roof of a ship. Signal from the antenna was split and supplied to six receivers. The correction data of Marine-VRS were received from a VRS Center. The all raw data and NMEA GPGGA data are logged.

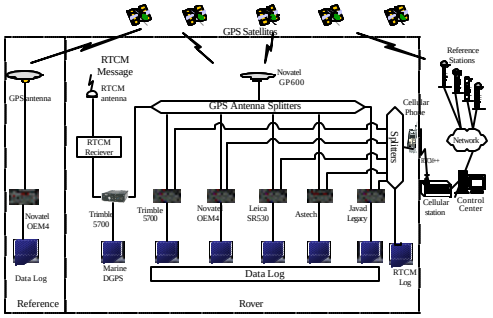

Figure 3. Experiment Set-up

The experiment includes two stages: docking in berth and sailing from TUMM to Rainbow Bridge. The baseline of Marine-RTK is about 100 meters when ship docks in berth, and 3.5 km when ship sails from TUMM to Rainbow Bridge, respectively. It is about 30 minutes when ship docks in berth. When ship sails form TUMM to Rainbow Bridge, four bridges are encountered.

3.2 Analysis of Results

3.2.1 Docking in berth

The satellite number in view is shown in Figure 4. There are about eight satellites in view when ship docks in berth.

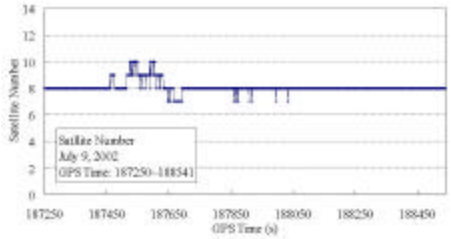

Figure 4. Satellite number

Figure 5 shows the cycle slip. The dot points denote cycle slip occurred. Satellite No. 4, 17 and 27 have cycle slips.

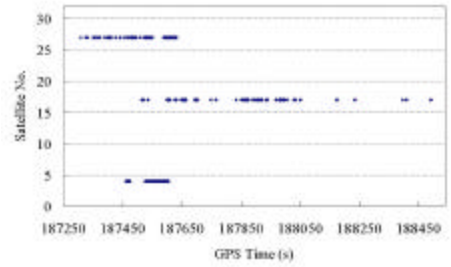

Figure 5. Cycle slip

The positioning results are shown in Figure 6 and Figure 7.

As shown in Figure 6, the ship drifts with wave. The compare of altitude variation between Marine-RTK and Marine-VRS are shown in Figure 7. The altitudes of antenna vary with water level. Marine-RTK and Marine-VRS have same trend of variation.

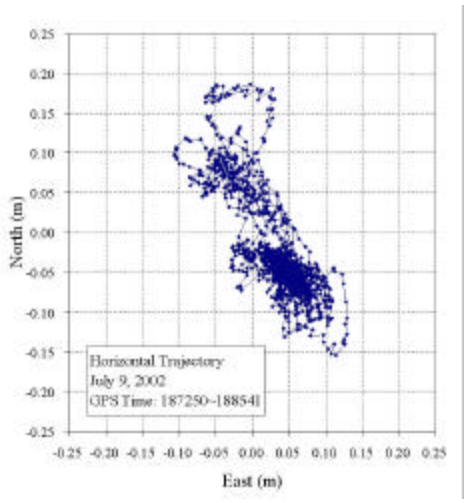

Figure 6. Horizontal trajectory (Marine-RTK)

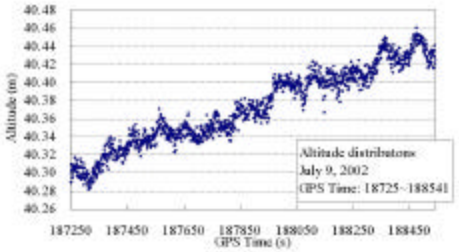

(a) Marine-RTK

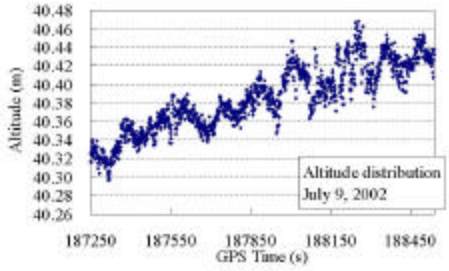

(b) Marine-VRS (Novatel)

Figure 7. Vertical variation

3.2.2 Sailing from TUMM to Rainbow Bridge

Because the data of Javad and Trimble are missed in Marine-VRS experiment when ship sails from TUMM to Rainbow Bridge, the results of Marine-RTK are only compared with the results of Novatel, Astech and Leica receiver in Marine-VRS.

The satellite number in view when ship sails from TUMM to Rainbow Bridge is shown in Figure 8. The satellites are blocked four times when ship passed through four bridges.

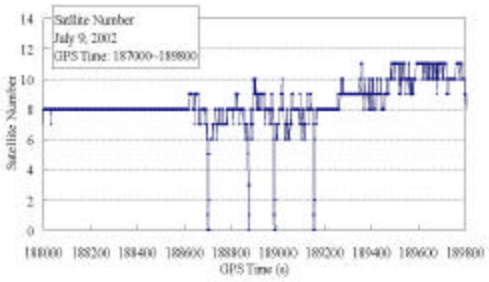

Figure 8. Satellite number

Figure 9 shows the cycle slip. There are a lot of cycle slip occurred, because of multipath and signal blocking.

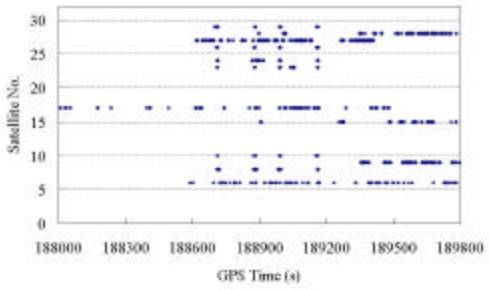

Figure 9. Cycle slip

The horizontal trajectory of antenna is shown in Figure 10.

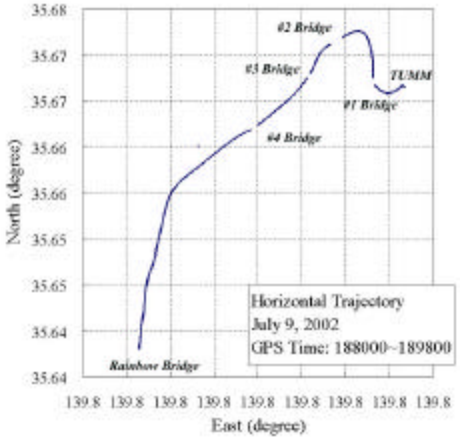

Figure 10. Trajectory of the Antenna

Altitude variations of antenna are shown in Figure 11. The variation of Marine-RTK is similar to the variation of Marine-VRS. Because the wave becomes stronger and stronger when the ship sails from TUMM to Rainbow Bridge, and the altitudes of antenna vary with the wave, the variation ranges of altitude became larger and larger.

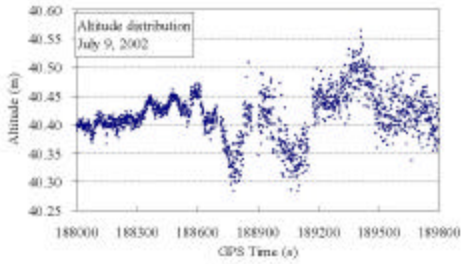

(a) Marine RTK

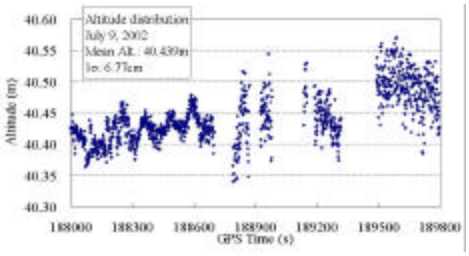

(b) Marine VRS (Novatel)

Figure 11. Vertical distribution

Figure 12 show altitude variation during passing through the four bridges. The time to fix of Marine-RTK is short than Marine-VRS.

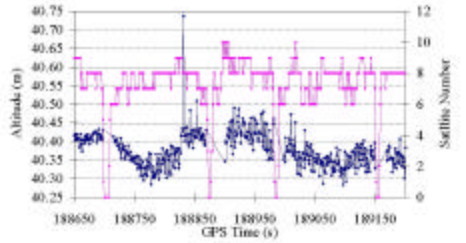

(a) Marine-RTK

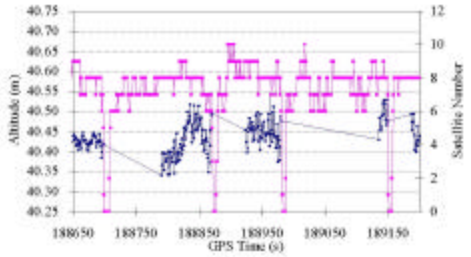

(b) Maine-VRS (Fixed)

Figure 12. Altitude distribution after passing through four bridges.

The time to fix after passing through bridges are summarized in Table 1. For Marine-RTK, the time to fix are about one second with altitude aiding, but 11 seconds without altitude aiding. The time to fix of Marine-RTK is less than Marine-VRS. Because the satellites in view after passing under second bridge are less

than other bridges, and the receiver lose track of the L2 signal sometimes, the time to fix after passing under second bridge with altitude aiding is longer than other bridges.

Table 1 Time to fix after passing under bridges (sec.)

	Bridges	1	2	3	4
Marine -RTK	Altitude-Aiding	1	6	1	1
	No-Altitude-Aiding	11	11	24	1
Marine -VRS	Novatel	75	35	138	18
	Astech	33	16	18	20
	Leica	19	32	23	18

The fixed percentages are summarized in Table 2. The fixed percentages of Marine-RTK are 97.5% with altitude aiding and 95.3% without altitude aiding. The fixed percentage with altitude aiding is larger than without altitude aiding. The fixed percentage of Marine-RTK is larger than Marine-VRS.

Table 2 Fixed Percentages

		Fixed Percentage* (%)
Marine -RTK	Altitude-Aiding	97.5
	No-Altitude-Aiding	95.3
Marin -VRS	Novatel	81.2
	Astech	90.6
	Leica	92.1

$$*: Fixed\ \ Percentage = \frac{Ambiguity\ \ Fixed\ \ Epoches}{Total\ \ Epoches} \times 100\%$$

The times to fix with altitude aiding are less than without altitude aiding, and the fixed percentages with altitude aiding are larger than without altitude aiding. As a result, it is helpful to use altitude aiding in ambiguities resolution.

4. Conclusion

A new approach using altitude aiding and using a wide-lane search before stepping to L1 ambiguity search technique in the marine environment has been investigated. Some tests were performed in order to assess the efficiency and reliability of approach, and a considerably good performance are achieved. The ambiguity fixed percentage was demonstrated 95.3% without altitude aiding and 97.5% with altitude aiding. The time to fix is almost single epoch with altitude aiding.

References

[1] Falin WU, Nobuaki KUBO, Akio YASUDA, Hiromune NAMIE and Hakjin KIM, Marine RTK-GPS Positioning in Tokyo Bay Using Virtual Reference Station(VRS) System, ENC-GNSS 2002, 2002.

[2] Toshiaki Tsujii, Masaaki Murata, Masatoshi Harigae, Takatsugu Ono and Toshiharu Inagaki, *Development of Kinematic GPS Software, KINGS, and Flight Test Evaluation*, Technical Report of National Aerospace Laboratory, 1998.

[3] Pratap Misra and Per Enge, GLOBAL POSITIONING SYSTEM, Signals, Measurements, and Performance, pp. 227-230, Ganga-Jamuna Press, 2001.

[4] James W. Sinko, *Single-Epoch Ambiguity Resolution for Highway and Racetrack Applications*, ION GPS 2001, 2001.